

A flexible forecasting model for production systems

R. Hosseini, K. Yang, A. Chen, S. Patra,
Linkedin Data Science Applied Research Team

Abstract

This paper discusses desirable properties of forecasting models in production systems. It then develops a family of models which are designed to satisfy these properties: highly customizable to capture complex patterns; accommodates a large variety of objectives; has interpretable components; produces robust results; has automatic changepoint detection for trend and seasonality; and runs fast – making it a good choice for reliable and scalable production systems. The model allows for seasonality at various time scales, events/holidays, and change points in trend and seasonality. The volatility is fitted separately to maintain flexibility and speed and is allowed to be a function of specified features.

1 Introduction

Forecasting business metrics and quantifying their volatility is of paramount importance for many industries, including the technology industry. Long-term forecasts can inform the company executives about expectations about future growth (e.g. daily active users) or about future resource requirements (e.g. server capacity needed). Short-term forecasts with uncertainty intervals can be used to detect anomalies in the system, by comparing the forecasts with observed values.

The area of forecasting time series has a long history with many models and techniques developed in the past decades. Some important examples include: Classical time series models such as ARIMA (e.g. Hyndman and Athanasopoulos (2014)) and GARCH (Tsay (2010)); Exponential Smoothing Based methods (see Winters (1960)); State-space models (see Kalman (1960), Durbin and Koopman (2012), West and Harrison (1997)); Generalized Linear Models extensions to time series (Kedem and Fokianos (2002), Hosseini et al. (2015a)); Deep Learning based models such as LSTM (Hochreiter et al. (1997)). Our framework utilizes the powerful aspects of these various models. We provide more details below, after discussing the motivations for its development.

Here we discuss the desirable properties of a forecasting method in practice, especially for production systems in the technology industry. These properties are the motivation for our framework.

- Flexibility to accommodate complex patterns for the metric of interest: Flexibility is needed to achieve high accuracy. For example, in practice, often the growth can differ for weekdays versus weekends for a daily metric and this needs to be taken into account explicitly or implicitly to achieve accurate forecasts.
- Flexibility in the objective: As an example, depending on the application, the user might intend to capture the average values well (e.g. in Revenue forecasting) or the peak values well (e.g. in capacity planning).

- **Interpretability:** This can benefit users to inspect and validate forecasting models with expert knowledge. As an example, if the model is able to decompose the forecast into various components (e.g. seasonal, long-term growth, holidays), the users can inspect those components not only to validate the models but also to get insights about the dynamics of the metric.
- **Robustness:** It is important for the forecast values to be robust and have low chance of returning values which are implausible. This can indeed occur in the time series context for various reasons, including the divergence of the simulated values (see e.g. Hosseini et al. (2015a)).
- **Speed:** In many applications it is important to quickly train the model and produce forecasts. Speed can help with auto-tuning over parameter spaces and producing a massive number of forecasts, even when there are many training data points.

In our model, we have decomposed the problem into two phases:

- Phase (1) the conditional mean model;
- Phase (2) the volatility / error model.

In (1) a fitted model is utilized to predict the metric of interest and in (2) a volatility model is fitted to the residuals. This choice helps us with flexibility and speed as integrated models are often more susceptible to being poorly tractable (convergence issues for parameter estimates), and demonstrate divergence issues when Monte Carlo Methods are used to generate future values, which is the case for many of the aforementioned methods such State-Space Models or GLM based models (Tong (1990), Hosseini et al. (2017)). As an example, estimating a model with complex conditional mean and complex volatility (i.e. with a large number of parameters) can run into stability and speed issues (Hosseini and Hosseini (2020)).

Phase (1) can be broken down to these steps:

- (1.a) extract raw features from timestamps, events data and history of the series;
- (1.b) transform the features to basis functions;
- (1.c) apply a change-point detection algorithm to the data to discover changes in the trend and seasonality over time;
- (1.d) apply an appropriate machine learning algorithm to fit those features (depending on objective).

Note that, the purpose of Step (1.b) is to transform the features into a space which can be used in “additive” models when interpretability is needed. For Step (1.d), our recommended choices are explicit regularization based algorithms such as Ridge. Note that if the objective is to predict peaks, quantile regression or its regularized versions are desirable choices. In the next sections,

we provide more details on how these various features are built to capture various properties of the series.

In Phase (2), a simple conditional variance model can be fitted to the residuals which allows for the forecast volatility to be a function of specified factors (e.g. day of week, if volatility depends on that).

The main contribution of this work is to develop a model which combines various techniques to achieve a highly customizable model which can run fast; have interpretable options and support variable objectives. Our events model is very flexible and allows for the deviation due to events to be of arbitrary shape even within a day. Also the regularization-based change-point algorithm is a novel method which can capture changes in both trends and seasonality – we demonstrate it works well in practice.

The paper is organized as follows. Section 2 discusses the model details. Section 3 provides the details for the automatic change-point detection component. Section 4 demonstrate how our models work using a particular use case. In Section 5, we discuss methodology for assessing performance of the models in terms of accuracy and in cross-validation. We also compare the performance of our models with some widely used open source libraries. Finally Section 6 concludes with a summary and discussion of possible extensions.

2 Conditional Mean and Volatility Models

This section discusses the details of our model. We refer to our model as Silverkite for clarity in the following.

First, we introduce the mathematical notation. Suppose $\{Y(t)\}, t = 0, 1, \dots$ is a real-valued time series where t denotes time. We denote the available information up to time t by $\mathcal{F}(t)$. We assume this information is given in terms of a covariate process, denoted by $\mathbf{Z}(t)$, as discussed in Kedem and Fokianos (2002). The covariate process is assumed to be a multivariate real-valued process and encodes the features to be utilized in the models. For example, we can consider the covariate process:

$$\mathbf{Z}(t - 1) = (1, Y(t - 1), Y(t - 2)),$$

which means the features used in the model are simply a constant and two lags. (This corresponds to a simple auto-regressive model of order 2, if we further assume that the conditional mean is linear and the conditional distribution is Gaussian.)

Figure 1 illustrates the model components diagram where the (sky) blue square nodes show the compute nodes; the green parallelograms show the (potential) user inputs; the dark cylinders show the (potential) input databases such as country holidays; the yellow clouds show the inline comment / descriptions.

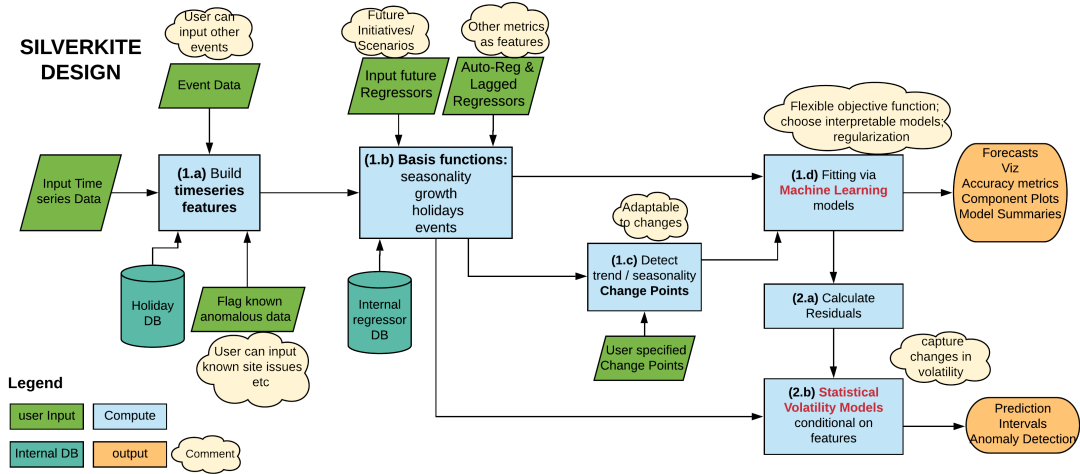


Figure 1: This diagram summarizes the steps involved in the Silverkite Algorithm. The square blue notes represents the computational nodes and include a number which represent the step. The nodes (1.a) to (1.d) correspond to Phase (1) which is the conditional mean phase. The nodes (2.a) and (2.b) correspond to Phase (2) which is the volatility / error model.

As we discussed in the introduction, the algorithm has two main phases.

- Phase (1): The conditional mean model
- Phase (2): The volatility / error model, fitted to residuals

As we discussed, this choice is made deliberately to increase the flexibility of the model in capturing complex mean patterns / objectives in modeling the mean and overall speed of the algorithm. The main reason is models which encapsulate the mean parameters and volatility parameters into one model often require slow Maximum Likelihood Estimation (e.g. in Hosseini et al. (2015a)) or intensive Bayesian computation (e.g. West and Harrison (1997)) due to parametric form of the volatility.

The conditional mean component

The very first step in building the model is generating the raw features. Here are some examples of raw features:

- Time of day (TOD): This is a continuous measure of what time in the day t is, in hour units, and ranges from 0 to 24. For example 12.5 is half past noon.
- Day of week (DOW): Categorical variable denoting day of week, from Sunday (0) to Saturday (7).

- Time of week (TOW): This is a continuous measure of when in the week t is, in day units, starting from Sunday. For example, 1.5 denotes Monday at noon.
- Time of year (TOY): This is a continuous measure of when in the year t is, in year units and ranges from 0 to 1. For example 1.5/365 denotes the second of January at noon in a non-leap year.
- Time of month (TOM) and time of quarter (TOQ) can be defined similarly and range from 0 to 1.
- Event / holiday labels: assume a holiday or re-occurring events database is available. For example, timestamps on January 1st could be labeled with “New Year”. Custom events can also be treated in the same way. If multiple event databases are relevant (e.g. Gregorian and Lunar calendar), multiple features are to be generated per database.
- Continuous Time (CT): This is a variable which measures the time elapsed from a particular date in year units. Typically, the reference date is the beginning of the time series, so that the first time point has value 0. For example if the series starts on Jan 1st, 2015, then end of 2016 will have the value of 2 since two years have elapsed.

Seasonality

The seasonality in a time series can appear in various time-scales. For example for hourly data, one can expect a periodic daily pattern across the day, a periodic weekly pattern across the week, and similarly periodic patterns across month, quarter and year.

We use Fourier series as the primary tool for modeling seasonality in various scales. For example for hourly data and within day variations, we use Fourier terms of the form:

$$s_k = \sin(k\omega_d d(t)), \quad c_k = \cos(k\omega_d d(t)), \quad \omega_d = 2\pi/24,$$

$$k = 1, \dots, K$$

where $d(t)$ denotes TOD (time of day), discussed above; and K is the appropriate order of Fourier series which can be determined in a Model Selection Phase. Note that the frequency ω_d is set to be $2\pi/24$ since TOD changes from 0 to 24. Similarly, we can define appropriate Fourier Series for weekly, monthly, quarterly and annual periodicity.

Growth

In order to model growth, we introduce some basis functions and allow for piece-wise continuous versions of those functions. By slight abuse of notation let t denote the continuous time (CT) introduced in the raw features. Then consider the following basis functions:

$$f(t) = t^p, \quad p = 1/3, 1/2, 1, 2, 3.$$

We allow for the growth to change with time continuously at given change-points t_1, \dots, t_k . Given the change-points and a basis function $f(t)$, we define

$$growth(t) = \alpha_0 f(t) + \sum_{i=1}^k \alpha_i 1_{t > t_i} (f(t) - f(t_i))$$

Note that $growth(t)$ is a continuous function of t , but allows the derivative of the function to change at the change-points.

In some forecast applications, we might have external information about the change-points, which can then be fed to the algorithm. However, in other applications such information might be unavailable or the growth shape might not conform to any such basis function. Therefore Section 3 presents a method for automatic change-point detection both for growth and seasonality.

Events and holidays

Here we present a method for modeling reoccurring events. This approach allows the period of the event to take any possible deviation from general trends. It assumes the impact of the event does not vary over time.

A prime example of such events are national/religious holidays in various countries and the days surrounding those holidays.

Suppose, the event occurs in the known periods $[t_i, t_i + l]$, where each i corresponds to a single occurrence of the event. Define the event time-coverage of the re-occurring event e to be:

$$TC(e) = \cup_i [t_i, t_i + l], \quad i \in \{1, 2, \dots\}$$

Then we define the basis function:

$$s_k(t; e) = \begin{cases} 0 & t \notin TC(e) \\ \sin(2\pi(t - t_i)/l) & t \in TC(e) \end{cases}$$

Similarly, we define $c_k(t; e)$ as the cosine counterpart.

In order to model the effects of event e , we add the basis functions

$$\{s_k(t; e), c_k(t; e), k = 1, \dots, k_e\},$$

where k_e is the appropriate Fourier Series order, to the set of basis functions.

Note that for a holiday e , the time coverage can be defined to include an expanded window surrounding that holiday instead of solely the holiday.

Moreover, when $\{K = k_e\}$ (same Fourier order used for seasonality as for the holiday), the basis functions can be expressed as interaction terms e.g.

$$s_k(t; e) = s_k(t) * \mathbb{1}_{TC(e)},$$

where $\mathbb{1}_{TC(e)}$ is the indicator function.

Remaining Temporal Dependence

After taking into account trends, seasonality, events, change-points (discussed in the next section), and other important features, often the residuals still show a temporal dependence (albeit often orders of magnitudes smaller than the original series). The remaining temporal correlation can be exploited to improve the forecast especially for short-term forecast horizons. We allow for an auto-regressive structure in the model e.g. by including lags in the model: $Y(t-1), \dots, Y(t-r)$ for some appropriate r .

While auto-regression can account for the remaining correlation in the series, for many applications a large r might be needed to capture long-term dependence in the chain. To remedy this issue, Hosseini et al. (2011b) suggested a technique to develop parsimonious models by aggregating the lags. As an example, for a daily series, consider the averaged lag series

$$AVG(Y(t); 1, 2, \dots, 7) = \sum_{i=1}^7 Y(t-i)/7.$$

This covariate then represent the average value for the value of the series over the past week. As another example, consider

$$AVG(Y(t); 7, 7 \times 2, 7 \times 3) = \sum_{i \in \{1, 2, 3\}} Y(t-7i)/3.$$

This covariate represent the average value of the series on the same day of week in the past 3 weeks. Similar series can be defined for other frequencies as well.

Lagged regressors and regressors

Suppose p other time series are provided with the same frequency as the target time series to forecast: $\mathbf{X}(t) = X_1(t), \dots, X_p(t)$. If such other metrics are available while future values are unknown, one can still use their lags in the models, similar to previous sections.

In the case that the future values of these variables are known, or can be forecasted reliably based on other models, we can directly use $X_1(t), \dots, X_p(t)$ as regressors. This also has applications in scenario-based forecasting where some underlying variables are to behave differently into the future.

Accommodating complex patterns

One of the advantages of our model compared to many commonly used models in practice is the ability to easily accommodate complex patterns. This is done by specifying interactions (between features). To mitigate the risk of the model becoming degenerate or over-fitting, regularization can be used in the machine learning fitting algorithm for the conditional model (e.g. Ridge). In fact, regularization also helps in minimizing the risk of divergence of the simulations of future series for the model which are discussed in Hosseini and Hosseini (2020).

Here we provide some examples of how complex patterns can be accommodated with interactions.

- Growth is different on weekdays and weekends. This is possible and unobserved in many series of interest. For example it could be the case that the usage of a particular app surges much more rapidly on weekends as compared to weekdays. Suppose the time frequency is daily and the model includes the categorical term DOW to model the weekly patterns. To accommodate this pattern we can interact the growth term e.g. $f(t) = t$ with DOW:

$$f(t) * DOW$$

where $*$ denotes the interaction as commonly used in standard softwares such as R (<https://www.R-project.org/>) or Python’s patsy package (<https://patsy.readthedocs.io/>). If a Fourier series is used to model weekly patterns, then one can interact the Fourier series terms or a subset of it with the growth function.

- Different months have different patterns for day of week. It might be possible that during different times of the year, the weekly patterns differ. Then one can use this interaction:

$$f(t) * month$$

where *month* is a categorical variable denoting the month of the year. Similar interactions can be considered if Fourier series are used to model the annual trends.

2.1 The volatility component

As discussed in the introduction, we elect to separately fit the conditional mean model and the volatility / error model. Integrated models of course can be considered where the model includes all components (e.g. Hosseini et al. (2015a) or West and Harrison (1997)).

In theory, the advantage of an integrated model is accounting for all uncertainty in one model. However, we consider a two-component model for the following reason: (a) more flexibility in the mean components model in terms of features and algorithm; (b) more flexibility in the volatility model; (c) considerable speed gain by avoiding computationally heavy Maximum Likelihood Estimation (e.g. Hosseini et al. (2015a)) or Monte Carlo Methods (e.g. West and Harrison (1997)). These factors are very important in a production environment where often fast and reliable forecasts are needed. The increased reliability is due to (a) more stable / robust estimates of the model parameters (b) less chance of the forecasted values into the future to diverge to unreasonable values (as reported by Tong (1990) and Hosseini and Hosseini (2020)).

Here we discuss the details for the volatility model. Suppose $Y(t)$ is the target series and $\hat{Y}(t)$ is the forecasted series. Then define the residual series as follows:

$$R(t) = Y(t) - \hat{Y}(t)$$

Assume the volatility depends on given categorical features F_1, \dots, F_p which are also known into the future. As an example, these features could be the raw time features defined previously such as “Day of week (DOW)” or “Is Holiday” which determines if time t is a holiday or not. Then given

any combination of features F_1, \dots, F_p , we consider the empirical distribution $(R|F_1, \dots, F_p)$ and fit a parametric or non-parametric distribution to the combination as long as the sample size for that combination, denoted by $n(F_1, \dots, F_p)$ is sufficiently large e.g. $n(F_1, \dots, F_p) > N$, $N = 20$. Note that one can find an appropriate N using data e.g. during cross-validation steps by monitoring the distribution of the residuals. Then from this distribution, we estimate the quantiles: $Q(F_1, \dots, F_p)$ to form the 95% prediction interval:

$$\hat{Y}(t) + Q(F_1, \dots, F_p)(0.025), \hat{Y}(t) + Q(F_1, \dots, F_p)(0.0975),$$

and similarly for other prediction intervals. One choice for a parametric distribution is the Gaussian distribution $\mathcal{N}(0, \sigma^2(F_1, \dots, F_p))$ which can be appropriate for some uses cases. The reason, that we have forced the mean to be zero is, we do not want to volatility model to modify the forecasted value which is the result of often much more complex mean model with many more features. Regarding normality assumption, note that while the original series can be heavily skewed, it could be the case that the residual series is close to normal, especially after conditioning on F_1, \dots, F_p . For use cases where the normality of the conditional residuals is not reasonable, we can use non-parametric estimates of the quantiles using various approaches e.g. by simply calculating sample quantiles for sufficiently large samples.

We also need to address the case where the sample size for a given combination is smaller than N . In this case, we need to fall back to another reasonable way to come up with prediction interval. To determine the fall back values: we calculate the Interquartile Range $IQR(c) = (Q(0.75) - Q(0.25))$ for each combination c ; then order these IQR increasingly and for a large $p \in [0, 1]$, e.g. $p = 0.9$, we pick c_0 which attains that IQR. Then we use the quantiles of c_0 as the fall back value. The idea behind this approach is to fall back to some quantiles which are coming from more variable combinations. Note that in practice, the combinations should be chosen in a way that no fall-back is necessary and this mechanism is only there to cover rare cases when a combination gets assigned smaller sample sizes. For future work, one can also consider parametric models for volatility in residuals to be able to accommodate a large number of features in volatility. The concrete steps for fitting the volatility model are described in Algorithm 1.

Algorithm 1: Volatility algorithm

Data: Apply the forecast model to generate predictions

Calculate residuals

Split data based on feature values

Estimate distribution for large combinations

Consider combinations C_{large} with sample size $\geq N$;

for combination c in C_{large} **do**

 Calculate $IQR(c)$

 Calculate desired lower and upper bounds: $q_1(c), q_2(c)$

end

Estimate fall-back volatility for small combinations

Order the combinations C_{large} with respect to $IQR(c)$.

Find the combination, c_0 , which is percentile of p in C_{large} .

Set fall back quantiles to $q_1(c_0), q_2(c_0)$.

Consider combinations C_{small} with sample size $< N$;

for combination c in C_{small} **do**

 Set lower and upper bounds to the fall back quantiles

end

Result: Return $(q_1(c), q_2(c))$ for all c ; and fall back quantiles $q_1(c_0), q_2(c_0)$

3 Changepoint Detection

Changepoints play an important role in forecasting problems. By a changepoint, we refer to a time point in a time series, with the pattern in the data segment after the time point exhibiting a change from the data segment prior to it. Capturing the changepoints can help the model adapt to the most recent data patterns and learn the right behavior in forecasts. This section discusses a changepoint detection algorithm that focuses on trend changepoints. The algorithm is based on the adaptive lasso (Zou, 2006) to select significant changepoints from a large number of potential changepoints. While fully automatic detection is possible, tuning parameters are provided to allow flexibility.

3.1 Trend Changepoint Detection

The trend of a time series describes the long-term growth that ignores seasonal effects or short-term fluctuations. As discussed in Subsection 2, in general the trend can be denoted as a function of time, i.e.,

$$\text{long-term trend} = g(t)$$

for a continuous function g . This growth function can be approximated with basis functions such as linear, quadratic, cubic and logistic. Here, we focus on the case with linear basis functions as it suffices to be a good starting point for most applications we have encountered. In fact, according

to the Stone-Weierstrass Theorem (Chapter 7 of Rudin (1976)), any continuous function can be approximated by a piece-wise linear functions. (Note however, this does not imply that there are no merits in considering other basis functions in other applications, as other basis functions could potentially capture some complex trends more parsimoniously, but we do not discuss that here further for brevity.)

Given a list of changepoints t_1, \dots, t_k , we can approximate the continuous function f with piece-wise linear function

$$g(t) = a_0 t + \sum_{i=1}^k a_i \mathbb{1}_{\{t > t_i\}}(t - t_i).$$

The approximation error gets smaller when we have more changepoints, while the risk of over-fitting also gets higher, thus making the forecast less reliable. Therefore, the method discussed here intends to only select significant trend changepoints. The proposed method here is a regularized regression based algorithm with a few filters being applied for practical considerations, and is able to identify significant trend changepoints. The steps of this procedure are given in algorithm 2.

First, we apply an optional aggregation. For example, aggregating daily data into weekly data. The main purpose of applying this aggregation is to eliminate short-term fluctuations. For example, a short holiday effect on daily data should not be picked up as long-term trend changes. Note that this aggregation process may not be necessary if data frequency is already sufficiently coarse e.g. for weekly data.

The next step is to place a fine regular grid of potential changepoints uniformly over the span of time of the series. For example for daily data with weekly aggregation, placing potential changepoints every week or every two weeks can be considered. However, it also would introduce false or pseudo changepoints. Therefore, a balanced approach is needed, which we will consider shortly. Large number of potential changepoints, also guarantees the existence of a potential changepoint, sufficiently close to any “true” trend changepoint.

We allow for some other restrictions in the procedure to find the appropriate change points. For example, we allow for the user to specify a period at the end of the series where no change point is allowed. The reasoning is that the position of last changepoint and its slope afterwards has a significant impact on the forecasted values. This way, we allow for expert knowledge of the nature of the series of interest to be incorporated into the model.

The core step applies the Adaptive Lasso (Zou, 2006) to the regression problem with the aggregated time series as the response and the changepoints and yearly seasonality as regressors, i.e.,

$$y_{t,agg} = a_0 t + \sum_{i=1}^k a_i \mathbb{1}_{\{t > t_i\}}(t - t_i) + \sum_{j=1}^K (\beta_{ci} c_j + \beta_{si} s_j), \quad (1)$$

where c_j and s_j are the sin and cosine functions corresponding to the yearly Fourier series, as

discussed in Subsection 2,

$$s_k = \sin(k\omega_y y(t)), c_k = \cos(k\omega_y y(t)), \omega_y = 2\pi, k = 1, \dots, K_1,$$

where $y(t)$ denotes TOY (time of year) defined in Subsection 2. The adaptive lasso adds weights to the L_1 norm penalization of the lasso (Tibshirani, 1996), where the weights are chosen based on various rules, for example, the reciprocal of some initial estimations of the coefficients. The reason that we use the adaptive lasso over the lasso is that the adaptive lasso can gain the desired sparsity level without over-shrinking the significant coefficients, with properly chosen weights, as discussed in Zou (2006). If the time series has a long history, yearly seasonality change may be falsely captured as trend change, so it's better to refit yearly seasonality after some period, e.g., every 2 years. In the regression formulation above, this can be handled by introducing extra regressors that account for yearly seasonality change, e.g.,

$$s_{k1} = \mathbb{1}_{\{t > t_1\}} \sin(k\omega_y y(t)), c_k = \mathbb{1}_{\{t > t_1\}} \cos(k\omega_y y(t)), \omega_y = 2\pi, k = 1, \dots, K_1,$$

for some change period t_1 . Introducing these terms will fit different yearly seasonality before and after t_1 .

Note that we should only penalize the changepoint parameters i.e.,

$$\begin{aligned} & \hat{a}_0, \dots, \hat{a}_k, \hat{\beta}_{c1}, \hat{\beta}_{s1}, \dots, \hat{\beta}_{cK}, \hat{\beta}_{sK} \\ = & \arg \min \sum_{m=1}^n \left[y_{t,agg} - \left(a_0 t + \sum_{i=1}^k a_i \mathbb{1}_{\{t > t_i\}} (t - t_i) + \sum_{j=1}^K (\beta_{ci} c_j + \beta_{si} s_j) \right) \right]^2 + \lambda \sum_{i=1}^k w_i |a_i|, \end{aligned} \quad (2)$$

for some weights $w_i, i = 1, \dots, k$. This partial penalized regression can be solved with a fast coordinate descent algorithm (Tseng, 2001). An alternative is to use projection to split the optimization problem into two steps. The first step fixes the L_1 -norm penalized coefficients and estimate the other coefficients as a ridge regression problem. The second step uses the estimated coefficients from the first step and reduce the problem into a Lasso regression problem. Both methods requires some math and programming. A derivation of the algorithm is given in appendix 7.1. It is worth noting that we are not losing too much by directly optimizing (1) over (2). The only difference is that penalizing the x_0 term brings in a pseudo-changepoint at the very beginning of the time series to “pick up” the baseline trend. This can be avoided by not allowing potential changepoints to be placed near the very beginning of the time series. Existing libraries such as *sklearn* (Pedregosa et al., 2011) can be utilized to solve the problem efficiently.

After the regularization, we have selected significant trend changepoints. However, there can be detected changepoints that are too close to each other. These types of changes usually account for consecutive changes or gradual changes. As for pure trend changepoint detection, the result does not need further handling. If one wants to use these changepoints as input for a forecast model and prefers parsimony, a rule-based post-filtering method can be applied to remove redundant trend changepoints.

Algorithm 2: The automatic trend changepoint detection algorithm.

Data: Time series data.

Pre-processing:

Aggregation (optional);
Put a large number of potential changepoints uniformly;
Eliminate the potential changepoints in forbidden region (e.g.;
the end);

Regularization:

Create trend features (including changepoints) and yearly seasonality features;
Fit a regression model with the features (initial estimation);
Compute feature weights;
Fit regression model with adaptive l_1 norm penalty on the changepoint features;

Post-processing:

Group selected changepoints with distance less than a threshold;
for *group in groups* **do**
 while *can add or remove changepoints* **do**
 Remove the changepoint with smaller change if two or more are too close;
 Trace back to see if any changepoint can be added back;
 end
end

Result: The detected trend changepoints.

Here we provide more details about filtering redundant change points. First, we group changepoints that are close to at least one another with respect to some threshold. For each group, we start with the first changepoint and look at the second one. The one with smaller changes are dropped, and we go to the third one, and so on. If we dropped the second changepoint, and the distance between the first and the third changepoints is greater than the threshold, we won't need to compare those two changepoints, and will continue to compare the third and the fourth changepoints. In a special case when $c_1 < c_2 < c_3$, where c_i is the magnitude of the i^{th} changepoint, after dropping the first and the second changepoints, the first changepoint can be added back, if the distance between the first and the third changepoints is large enough. Each time we remove a changepoint, we check back to see if any deleted changepoints can be added back. This rule-based filtering method not only enforces minimal distance to the detected trend changepoints, but also retains as many changepoints as possible.

Through the whole algorithm, the following components can be customized to fit specific use cases

- The aggregation frequency.
- The distance between potential changepoints or how many potential changepoints.

- The time period(s) with no change points.
- The yearly seasonality Fourier series order.
- How often yearly seasonality changes.
- The initial estimation method for adaptive Lasso.
- The regularization strength.
- The minimum distance between detected change points.
- Any customized trend change points to be added to detected change points.
- The minimum distance between a detected change point and a customized change point.

The above algorithm can stand alone as a trend change point detection algorithm. It runs fast and gives significant trend change points to help capture long-term events, product feature launches, changed in underlying dynamics, etc. On the other hand, the output can also be used to specify the trend change points as in Section 2. The advantage of detecting trend change points independently from performing it while fitting the model is to allow more flexible algorithms in the fitting phase, because it separates estimation for more interpretability, and makes it easier to tune sub-modules.

3.2 Seasonality Change point Detection

In some time series, seasonality effect can change over time similarly to trend. Product features and news events can increase or decrease the volatility of the time series. Gradual changes in volatility can be modeled with interactions, however, seasonality change points are a more flexible and automatic way to capture this effect.

Seasonality effect is modeled with Fourier series terms in the model, and this makes it easy to include seasonality change points. We use truncated seasonality features to capture seasonality changes. For every Fourier series term s_k and c_k , the truncated terms $s_k \mathbb{1}_{\{t > t_{scp}\}}$ and $c_k \mathbb{1}_{\{t > t_{scp}\}}$ models the change after a seasonality change point t_{scp} . A regularized regression can be used to choose significant seasonality change points from a large number of potential seasonality change points as we do in automatic trend change point detection.

The main difference between trend change points and seasonality change points lies on two parts. The first part is that the seasonality has multiple components, for example, yearly seasonality, quarterly seasonality, monthly seasonality, weekly seasonality, daily seasonality, etc. The second part is that for each component, there are multiple Fourier series bases that account for the same seasonality change point.

In our model, a group lasso type of regularization (Yuan, 2006) is used on the the Fourier bases for each potential change point of each component. This method drops all Fourier bases of one change point in one component entirely, however, the resulted seasonality is not smooth

because of the entire changes. Using L_1 -norm over all terms can still give the desired sparsity level and also gives smoother seasonality changes. Therefore, the same adaptive method discussed in trend changepoints also works for seasonality changepoint detection in practice.

4 Example application to bike-sharing data

This section demonstrates how various model components of our proposed model work through an example. We consider a dataset with hourly counts of rented bikes in a bike-sharing system.

The bike-sharing data include the hourly counts of rented bikes in Washington DC during 2011 to 2019 and were obtained from www.capitalbikeshare.com. We have also joined this data with daily weather data from a nearby station (BWI Marshall Airport). The weather data was downloaded from “Global Historical Climatology Network” (<https://www.ncdc.noaa.gov/>) and contains the daily minimum and maximum temperature and precipitation total.

Figure 2 shows the time series.

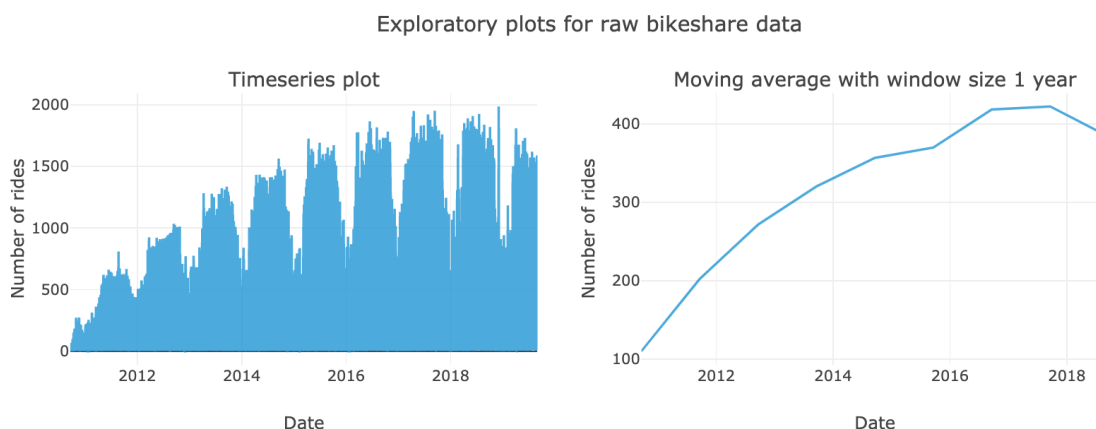


Figure 2: The raw time series (left) and the trend by a moving average of 365 days (right).

To build a Silverkite model, we will go over the components and try to find out what are the key components to be used in the model. First, the Right Panel in Figure 2 shows the rolling mean of the raw time series with a rolling window size of 24×365 (1 year). We observe that the trend is roughly increasing before late 2017 and starts to decrease after that. There are some slight growth rate changes but overall the trend can be modeled with a linear trend with changepoints.

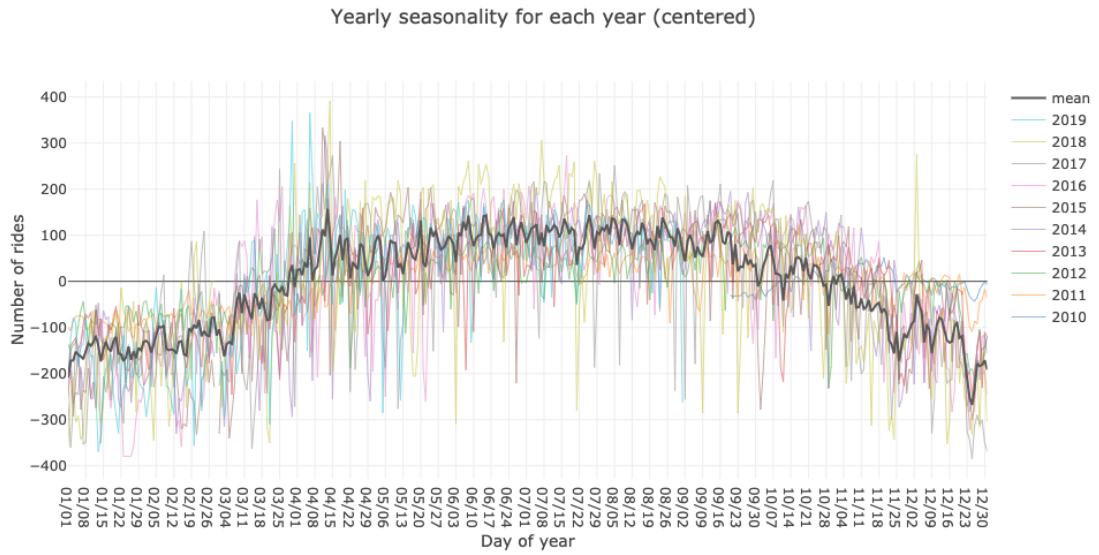


Figure 3: Yearly seasonality of the bike-sharing data.

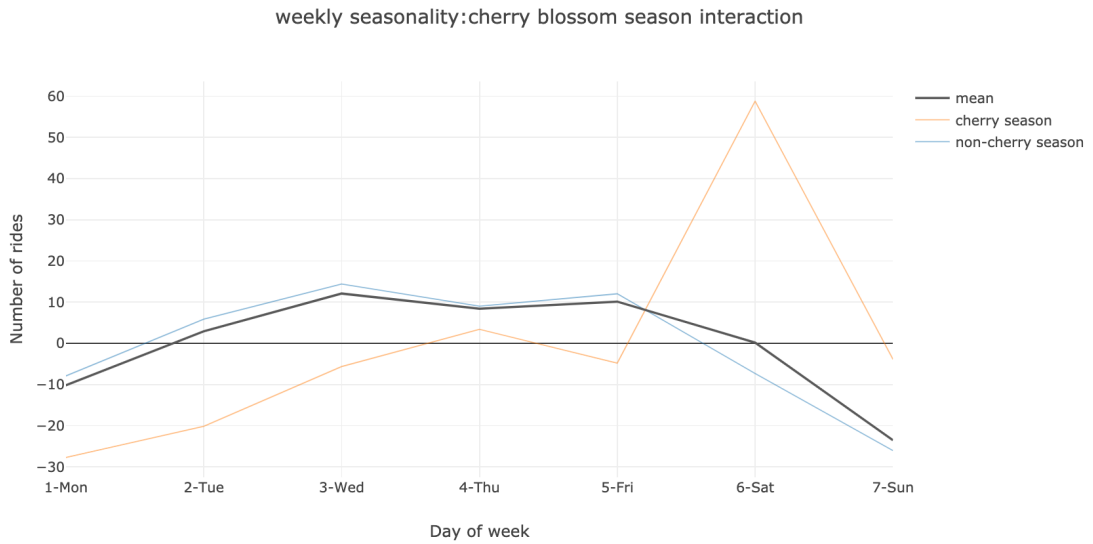


Figure 4: Different weekly seasonality for cherry season (Mar 20-Apr 30) and non-cherry season.

The seasonality components include different length of periods. We mainly focus on yearly seasonality, weekly seasonality and daily seasonality, because the other periods do not have appar-

ent patterns or convincing seasonal reasons. Figure 3 shows the yearly seasonality which indicates that there are more rides during warm months.

From the "mean" line in Figure 4, the weekly seasonality is not very clear at first. However, upon inspecting the weekly seasonality broken down by month, we observe that the weekly seasonality in April differs significantly from other months. The reason is that Washington DC has one of its most significant events around April – The Cherry Blossom Festival.

Figure 4 shows the contrast in weekly seasonality pattern between the Cherry Blossom Season (approximately March 20 – April 30) and the rest of the year. This observation can be modeled using an interaction between weekly seasonality and an indicator variable determining if the observation is in Cherry Blossom Season or not.

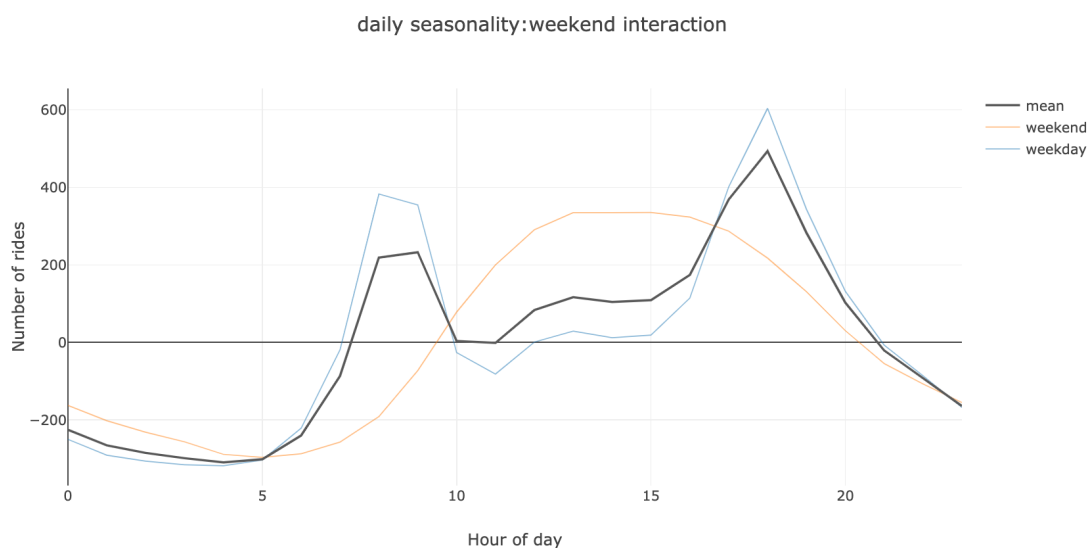


Figure 5: Different daily seasonality for week-days and weekend.

The daily seasonality patterns are very significant but differ on weekdays versus weekends. This is typical for time series that involve human activity. The daily seasonality effect interacting with weekend is shown in Figure 5. The figure suggests to differentiate between daily patterns of weekdays and weekends. This can be done in various ways, for example, by allowing for an interaction between seasonal daily patterns and a weekend indicator. Alternatively we could consider a sufficiently large number of Fourier series terms for a weekly pattern (or a combination of both).

The holiday effect is hard to see from component plots, but from Figure 3, we can see there are some small dips that are due to holidays.

In summary, the models will include the following components

- CT (continuous time to model the long-term trends)
- changepoints
- yearly seasonality
- weekly seasonality and its interaction with Cherry Blossom Season
- daily seasonality : weekend interaction
- holidays
- weather regressors
- autoregression

First we consider a forecast horizon of 24×14 (2 weeks). Because the number of rides is always non-negative, we clip negative values at zero. A linear growth is used as long-term trend function. For trend changepoints, we create a grid of potential changepoints every 15 days but skip the last 30 days (to avoid detecting artificial change points toward the end of the series). A yearly seasonality of order 15 is used in the changepoint detection algorithm. For the Lasso problem, it's easy to verify by KKT conditions that $\|\mathbf{X}^T \mathbf{y}\|_\infty / n$ is the minimal tuning parameter that corresponds to no non-zero coefficients. The regularization parameter, we use in detecting changepoints is 10^{-3} of that value, which provides moderate trend changepoints. An aggregation of 3 days is used for the changepoint detection aggregation process (Algorithm 2).

For seasonality, we use order 15, 3 and 12 for yearly, weekly and daily seasonality, respectively. Because the volatility changes over time as well, we also introduce seasonality changepoints, which allows seasonality components to refit after changes, however, the seasonality changepoints is not allowed within the last 365 days of data, to avoid a potentially poor fit of yearly seasonality.

A list of common holidays together with their plus/minus 1 day were created as separate indicators. We also include the two interaction groups we discussed above: weekly seasonality and Cherry-Blossom Season indicator; daily seasonality and weekend indicator.

Figure 6 compares the forecast with the actual data during the test period, which is located at the end of the time series. We can see that with our daily seasonality and weekend indicator interaction, the model is able to capture the bimodal daily seasonality on weekdays and unimodal daily seasonality on weekends. Figure 7 shows the detected trend and seasonality changepoints and the estimated trend in the model. It aligns with our expectations. Figure 8 shows the forecast versus the actual data around Thanksgiving 2018. From the figure, we see the holiday effect is picked up by the model, by observing that the number of rides is lower compared to regular non-holiday number of rides on the same weekday. Moreover, the interaction between whether it is weekend and daily seasonality also captures the uni-modal shape on these holidays (non-workdays). A gap in prediction happens on Nov 15 in the same plot. The reason is that Washington DC was hit with biggest November snowfall in 29 years, and people wasn't ready for a snow

riding commuting yet. We weren't explicitly capturing this effect so there is the gap, however, any knowledge-based observations can be modeled with extra regressors.

Autoregressive components are useful in picking up remaining trends which are not explained by seasonality, growth, events and change points. The effect of autoregression cannot be easily observed from figures. A cross-validation study is used to demonstrate its usefulness. The cross-validation includes 20 folds. The validation folds are taken from the end of the data set, with a 2-week window between each fold. The forecast horizon is set to 24 hours for short-term use case.

From the cross-validation study, we have an RMSE of 102.3 when including autoregressive components, compared to 123.0 when not including autoregressive components. Let $Y(t)$ be a time point in the forecast phase, the autoregressive terms used include $Y(t - 24)$, $Y(t - 25)$, $Y(t - 26)$ as autoregressive terms. They also include these three aggregated terms:

$$AVG(Y(t); 7 \times 24, 14 \times 24, 21 \times 24),$$

which is taking an average of observed values in the same hour of last three weeks.

$$AVG(Y(t); 24, 25, \dots, 191),$$

which is the average of the last 7 days; and

$$AVG(Y(t); 192, 193, \dots, 359)$$

which is the average of the week prior to last. These are the default choices (for hourly data with forecast horizon of 24) in our model and are not optimized for this use case in particular. However, the user can use grid search to optimize these choices further.

Note that the minimum lag used in the model is 24 which is the forecast horizon. This will assure that, at prediction time, all the lags used in the model to forecast are observed and not simulated. This sometimes can help with accuracy, and is also beneficial in terms of speed as we do not need to perform simulations at the prediction phase (to fill in the lags needed into the future). It is worth mentioning however, that the optimality of such choices depend on underlying use case and user should experiment with various models.

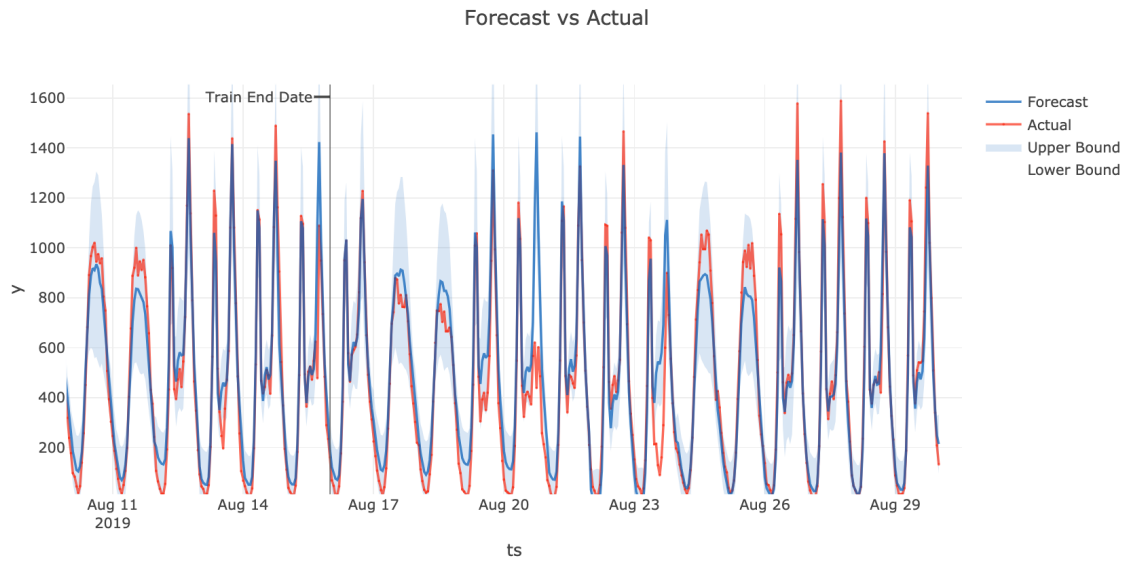


Figure 6: Forecast versus actual for Silverkite on bike-sharing data during test period.

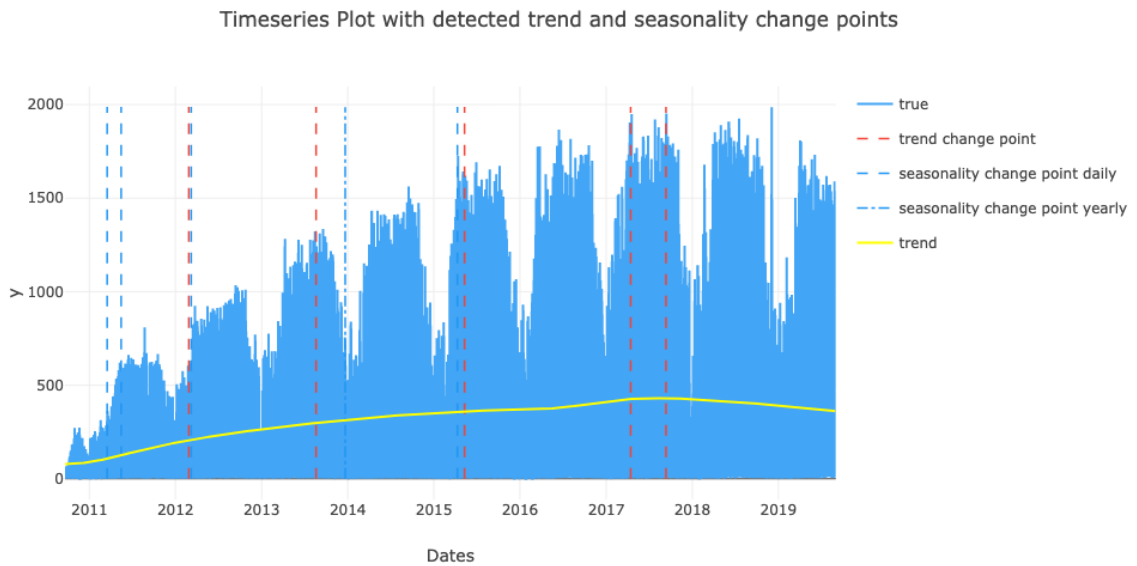


Figure 7: Detected trend and seasonality changepoints for bike-sharing data.

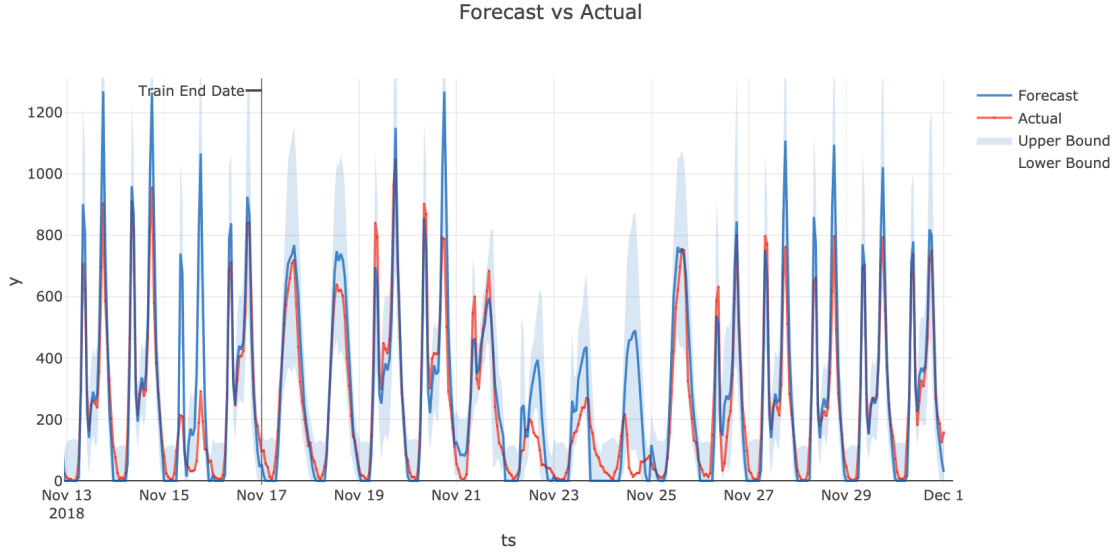


Figure 8: Forecast versus actual for Silverkite on bike-sharing data during Thanksgiving.

5 Assessment and Benchmarking

This section presents details on appropriate methods to assess the performance of forecasting algorithms in terms of accuracy.

To estimate how accurately a forecasting model (e.g. Silverkite) performs in practice, we use cross-validation (CV). Cross-validation is a technique for assessing how the results of a predictive model generalizes to new data. In the time series context the new data refers to values in the future. Below we describe an assessment method which is appropriate for forecasting applications.

We benchmark the prediction accuracy of Silverkite against that of popular state of the art algorithms such as Auto-Arima and (Facebook) Prophet. The prediction accuracy is measured by Mean Average Percentage Error (MAPE) which is defined as

$$\text{MAPE}(Y) = \sum_{t=1}^T \left| \frac{Y(t) - \hat{Y}(t)}{Y(t)} \right| \quad (3)$$

MAPE is more popular in applications as compared to RMSE (Root Mean Square Error), as it provides a relative (scale-free) measure of error compared to the observation.

We use a rolling window CV for our benchmarking, which closely resembles the well known K -fold CV method. In K -fold CV, the original data is randomly partitioned into K equal sized subsamples. A single subsample is held out as the validation data, and the model is trained

on the remaining $(K - 1)$ subsamples (Hastie et al. (2009)). The trained model is used to predict on the held-out validation set. This process is repeated K times so that each of the K subsamples is used exactly once as the validation set. Average testing error across all the K iterations provides an unbiased estimate of the true testing error of the machine learning (ML) model on the data.

Due to the temporal dependency in time-series data the standard K -fold CV is not appropriate. Choosing a hold-out set randomly has two fundamental issues in time series context:

1. Future data is utilized to predict the past.
2. Some time series models can not be trained realistically with a random sample, e.g. the autoregressive models due to missing lags.

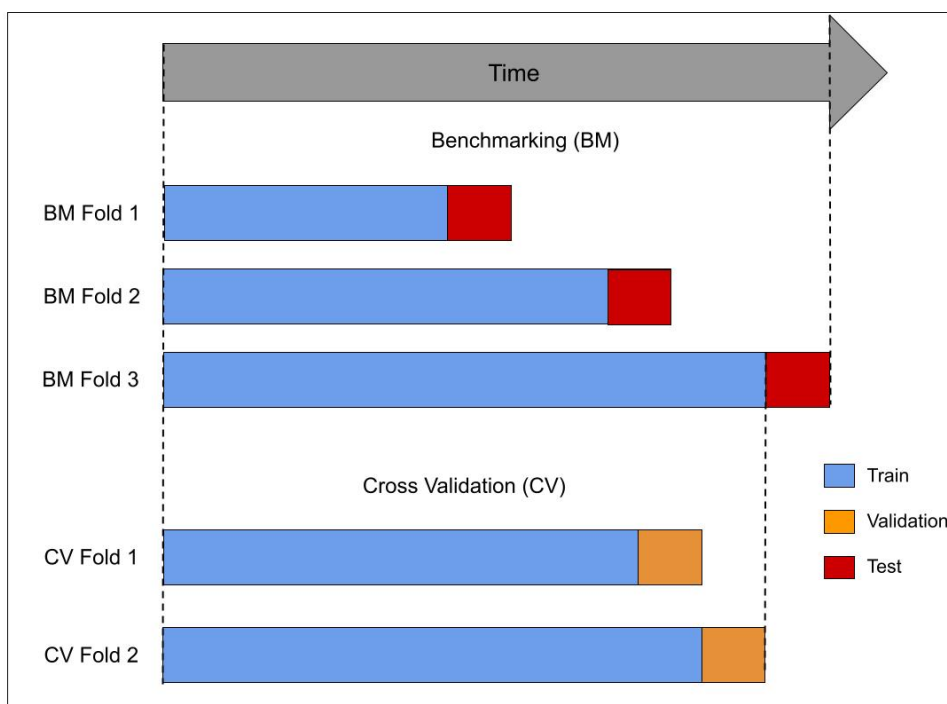


Figure 9: Fold structure for a Rolling Window Cross Validation. Expanding window configuration shown, where each training set has the same train start date.

Rolling window CV addresses this by creating a series of K test sets. For each test set, the observations prior to the test set are used as a training set. Within each training set, a series

of CV folds are created, each containing a validation set. For time consideration, we choose to create a single CV fold for each training set. Number of data points in every test and validation set equals forecast horizon (CV horizon in Table 1). Observations that occur prior to that of the validation set are used to train the models for the corresponding CV fold (Figure 9). Thus, no future observations can be used in constructing the forecast, either in validation or testing phase. The parameters minimizing average error on the validation sets are chosen. This model is then retrained on the training data for the corresponding becnh-mark (BM) fold. The average error across all test sets provides a robust estimate of the model performance with this forecast horizon.

Frequency	Forecast horizon	CV horizon	CV minimum train periods	Periods between splits	Number of splits
daily	1	1	365*2	25	16
daily	7	7	365*2	25	16

Table 1: Details about the parameters used for cross-validation (CV) during benchmarking

All the models are run on the 2 different forecast horizons (1 day and 7 day) for daily data sets (Table 1). These horizons roughly represent short-term, average-term forecasts for the corresponding frequency. We plan to publish more bench marking results on more data sets, more frequencies (e.g. hourly, weekly) and more time horizons in the future.

We require the datasets to have at least 2 years worth of training data so that the models can accurately estimate yearly seasonality patterns. The number of periods between successive test sets and total number of splits are chosen for each frequency to ensure the following:

1. The predictive performance of the models are measured over an year to ensure that cumulatively the test sets represent real data across time properties e.g. seasonality, holidays etc. For daily data, periods between splits(25) * max splits(16) = 400 > 365, hence the models are tested over a year.
2. The test sets are completely randomized in terms of time features. For daily data, setting “periods between splits” to any multiple of 7 results in the training and test set always ending on the same day of the week. This lack of randomization would have produced a biased estimate of the prediction performance. Similarly setting it to a multiple of 30 has the same problem for day of month. A gap of 25 days between test sets ensures that no such confounding factors are present.
3. Minimize total computation time while maintaining the previous points. For daily data, setting “periods between splits” to 1 and maximum number of splits to 365 is a more thorough CV procedure. But it increases the total computation time 25 fold and hence is avoided. We chose consistent benchmark settings suitable for all algorithms, including the slower ones.

We have used out-of-box configuration for Auto-Arima and (Facebook) Prophet and Silverkite. Silverkite uses a ridge regression to fit the model and contains linear growth, appropriate seasonality (e.g. quarterly, monthly and yearly seasonality for daily data), automatic changepoint

detection, holiday effects, autoregression, and daily and weekly seasonality interaction terms with trend and change points.

The benchmarking was run on three datasets for every forecast horizon.

- Peyton-Manning Dataset from fbprophet package (Facebook Prophet)
- Daily Australia Temperature Dataset, Temperature column
- Beijing PM2.5 Dataset

For consistency, no regressors were used for any dataset. The entire process is executed on a system equipped with 64 GB RAM and Intel Xeon Silver 4108 CPU @ 1.80 GHz. The CPU has 8 cores, each with 2 threads. The average test MAPE and runtime across datasets are summarized in Table 2. We can see that the default Silverkite MAPE is on par with Auto-Arima in short-term forecasts, outperforms other algorithms in average-term forecasts. However, Silverkite has a clear speed advantage over Prophet. This makes prototyping quicker in Silverkite and aids in building a customized more accurate model.

Note that the average test MAPE values are high due to values close to 0 in the Beijing PM2.5 dataset. These are a few benchmarks on public datasets. We plan to include more datasets, forecast horizons, and data frequencies that better match our industry applications and publish those results in the future.

Frequency	Forecast horizon	Test MAPE			Average Runtime (minute)		
		Silverkite	FbProphet	Auto-Arima	Silverkite	FbProphet	Auto-Arima
Daily	1	40.97	64.78	41.83	0.6	2.2	0.4
	7	53.52	56.98	55.82	0.6	2.2	0.5

Table 2: Summary of benchmarking results. MAPE and runtimes are averaged across multiple datasets.

6 Discussion

This paper introduced a flexible framework for forecasting which is designed for scalable and reliable forecasting in production environments (Section 5).

We showed how this design helps in generating flexible and interpretable forecasts as well as volatility estimates. As a particular example, the ability to use regularization algorithms as the training algorithm of the mean component, allows us to accommodate complex patterns in the model via feature interactions.

Having a separate volatility model, allows us to ensure fast speeds in production environments where updating the forecast for many series might be needed. However, this separation also helps in avoiding issues such as divergence of the simulated series which are a common issue when using integrated models (see Hosseini et al. (2015a) and Hosseini and Hosseini (2020)). The speed in fitting the model is also key in variable selection as many models can be fit to optimize the choice of the component and parameters e.g. the Fourier series order for various time-scales or the auto-regressive component complexity.

7 Appendix

7.1 Solving the Mixed Regularization Problem

In this subsection, we derive the two-step solution for the mixed penalty regression problem. Without loss of generality, we consider all weights equals 1, otherwise, the same formulation can be obtained with a re-scale on the design matrix and on the estimated coefficients. Consider the regression problem

$$\hat{\beta}_0, \hat{\beta}_1, \hat{\beta}_2 = \arg \min_{\beta_0, \beta_1, \beta_2} \|\mathbf{y} - \mathbf{X}_0\beta_0 - \mathbf{X}_1\beta_1 - \mathbf{X}_2\beta_2\|_2^2 + \lambda_1\|\beta_1\|_1 + \lambda_2\|\beta_2\|_2^2$$

Let,

$$\begin{aligned} \mathbf{X}_{02} &= [\mathbf{X}_0, \mathbf{X}_2] \\ \beta_{02} &= [\beta_0^T, \beta_2^T]^T \\ H_{02} &= \mathbf{X}_{02} (\mathbf{X}_{02}^T \mathbf{X}_{02})^{-1} \mathbf{X}_{02}^T \\ H_{\lambda 02} &= \mathbf{X}_{02} (\mathbf{X}_{02}^T \mathbf{X}_{02} + \lambda_2 \mathbf{D})^{-1} \mathbf{X}_{02}^T \end{aligned}$$

where \mathbf{D} is identity matrix with the first m diagonal entries equal to zero, and m is the number of columns in \mathbf{X}_0 . It's easy to verify that

$$\begin{aligned} H_{02} \mathbf{X}_0 &= \mathbf{X}_0 \\ H_{02} \mathbf{X}_2 &= \mathbf{X}_2 \end{aligned}$$

We have:

$$\begin{aligned} &\hat{\beta}_0, \hat{\beta}_1, \hat{\beta}_2 \\ &= \arg \min_{\beta_0, \beta_1, \beta_2} \|\mathbf{y} - \mathbf{X}_0\beta_0 - \mathbf{X}_1\beta_1 - \mathbf{X}_2\beta_2\|_2^2 + \lambda_1\|\beta_1\|_1 + \lambda_2\|\beta_2\|_2^2 \\ &= \arg \min_{\beta_0, \beta_1, \beta_2} \|H_{02}(\mathbf{y} - \mathbf{X}_1\beta_1) - \mathbf{X}_0\beta_0 - \mathbf{X}_2\beta_2 + (\mathbf{I} - H_{02})(\mathbf{y} - \mathbf{X}_1\beta_1)\|_2^2 + \lambda_1\|\beta_1\|_1 + \lambda_2\|\beta_2\|_2^2 \\ &= \arg \min_{\beta_0, \beta_1, \beta_2} \|H_{02}(\mathbf{y} - \mathbf{X}_1\beta_1) - \mathbf{X}_{02}\beta_{02}\|_2^2 + \|(\mathbf{I} - H_{02})(\mathbf{y} - \mathbf{X}_1\beta_1)\|_2^2 + \lambda_1\|\beta_1\|_1 + \lambda_2\|\beta_2\|_2^2 \\ &= \arg \min_{\beta_1} \arg \min_{\beta_{02}|\beta_1} \|H_{02}(\mathbf{y} - \mathbf{X}_1\beta_1) - \mathbf{X}_{02}\beta_{02}\|_2^2 + \|(\mathbf{I} - H_{02})(\mathbf{y} - \mathbf{X}_1\beta_1)\|_2^2 + \lambda_1\|\beta_1\|_1 + \lambda_2\|\beta_2\|_2^2 \end{aligned}$$

We have

$$\begin{aligned} \hat{\beta}_{02}|\beta_1 &= \arg \min_{\beta_{02}|\beta_1} \|H_{02}(\mathbf{y} - \mathbf{X}_1\beta_1) - \mathbf{X}_{02}\beta_{02}\|_2^2 + \|(\mathbf{I} - H_{02})(\mathbf{y} - \mathbf{X}_1\beta_1)\|_2^2 + \lambda_1\|\beta_1\|_1 + \lambda_2\|\beta_2\|_2^2 \\ &= \arg \min_{\beta_{02}|\beta_1} \|H_{02}(\mathbf{y} - \mathbf{X}_1\beta_1) - \mathbf{X}_{02}\beta_{02}\|_2^2 + \lambda_2\|\beta_2\|_2^2 \\ &= (\mathbf{X}_{02}^T \mathbf{X}_{02} + \lambda_2 \mathbf{D})^{-1} \mathbf{X}_{02}^T (\mathbf{y} - \mathbf{X}_1\beta_1) \end{aligned}$$

Plugging back into the original equation, we have

$$\begin{aligned}\hat{\beta}_1 &= \arg \min_{\beta_1} \|(H_{02} - H_{\lambda_{02}})(\mathbf{y} - \mathbf{X}_1\beta_1)\|_2^2 + \|(\mathbf{I} - H_{02})(\mathbf{y} - \mathbf{X}_1\beta_1)\|_2^2 + \lambda_1\|\beta_1\|_1 + \lambda_2\|\beta_2\|_2^2 \\ &= \arg \min \|(\mathbf{I} - H_{\lambda_{02}})(\mathbf{y} - \mathbf{X}_1\beta_1)\|_2^2 + \lambda_1\|\beta_1\|_1 \\ &= \arg \min \|(\mathbf{I} - H_{\lambda_{02}})\mathbf{y} - (\mathbf{I} - H_{\lambda_{02}})\mathbf{X}_1\beta_1\|_2^2 + \lambda_1\|\beta_1\|_1\end{aligned}$$

This can be solved with the conventional Lasso algorithm with:

$$\begin{aligned}X &= (\mathbf{I} - H_{\lambda_{02}})\mathbf{X}_1 \\ y &= (\mathbf{I} - H_{\lambda_{02}})\mathbf{y}\end{aligned}$$

References

- Brockwell, P. J., and Davis, R., A. (2016) *Introduction to Time Series and Forecasting: Edition 3*, Springer
- Durbin, J. and Koopman, S., J. (2012) *Time series analysis by state space methods*. Oxford University Press.
- Fokianos, K. (2012) Count Time Series Models *Handbook of Statistics, Volume 30, Chapter 12*, pp. 315–348 *Time Series Analysis: Methods and Applications* Edited by Rao, T. S., Rao, S. S. and Rao C.R.
- Hastie, T., Tibshirani, R. and Friedman, J. H. (2009) *The Elements of Statistical Learning*, Second Edition. Springer
- Hochreiter, S., and Schmidhuber, J. (1997). Long short-term memory. *Neural Computation*. 9(8): 1735–1780. doi:10.1162/neco.1997.9.8.1735. PMID 9377276. S2CID 1915014.
- Hosseini, R., Le, N. and Zidek, J. (2011b) Selecting a binary Markov model for a precipitation process. *Environmental and Ecological Statistics*, 18(4):795–820
- Hosseini, R., Le, N. and Zidek, J. (2012) Time-Varying Markov Models for Binary Temperature Series in Agrorisk Management. *Journal of Agricultural Biological and Ecological Statistics*, 17(2):283–305
- Hosseini, R., Takemura, A. and Hosseini, A. (2015a) Non-linear time-varying stochastic models for agroclimate risk assessment. *Environmental and Ecological Statistics*, 22(2):227–246.
- Hosseini, A., Hosseini, R., Zare-Mehrjerdi and Y., Abooie M. H. (2017) Capturing the time-dependence in the precipitation process for weather risk assessment. *Stochastic Environmental Research and Risk Assessment*, 31(3):609–627

- Hosseini, A., and Hosseini, R. (2020) Model selection for count time series with applications in forecasting number of trips in bike-sharing systems and its volatility arXiv:2011.08389
- Rob J. Hyndman, George Athanasopoulos (2014) *Forecasting: Principles and Practice*, OTexts, 2014 - Business forecasting - 291 pages
- Kalman, R.E. (1960) A new approach to linear filtering and prediction problems *Journal of Basic Engineering*, 82(1):35–45. doi:10.1115/1.3662552.
- Kedem, B., and Fokianos, K. (2002) *Regression Models for Time Series Analysis*, Wiley Series in Probability and Statistics
- Rudin, W. (1976) *Principles of mathematical analysis (3rd Edition)*, McGraw-Hill
- Schwartz, G. (1978) Estimating the dimension of a model. *Annals of Statistics*, 6:461–464.
- Thall, P. F. and Vail, S. C. (1990) Some covariance models for longitudinal count data with overdispersion *Biometrics*, 46(3):657–671
- Tibshirani, R. (1996) Regression shrinkage and selection via the lasso. *Journal of Royal Statistical Society B.*, 58(1):267–288.
- Tong, H. (1990) *Non-linear time series, a dynamical systems approach*. Oxford University Press
- Tsay, R., S. (2010) *Analysis of Financial Time Series, 3rd Edition* Wiley
- Tseng, P. (2001) Convergence of a block coordinate descent method for non-differentiable minimization *Journal of Optimization Theory and Applications*, 109(3):475–494
- Pedregosa, F., Varoquaux, G., Gramfort, A., Michel, V., Thirion, B., Grisel, O., Blondel, M., Prettenhofer, P., Weiss, R., Dubourg, V., Vanderplas, J., Passos, A., Cournapeau, D., Brucher, M., Perrot, M., and Duchesnay, E. (2011) Scikit-learn: Machine Learning in Python *Journal of Machine Learning Research*, 12:2825–2830
- Bias in error estimation when using cross-validation for model selection. *BMC Bioinformatics* 7, 91 (2006). <https://doi.org/10.1186/1471-2105-7-91>
- West, M. and Harrison, J. (1997) *Bayesian Forecasting and Dynamic Models, 2nd Edition*
- Winters, P. R. (1960) Forecasting Sales by Exponentially Weighted Moving Averages *Management Science*, 6(3):324–342, doi:10.1287/mnsc.6.3.324
- Yuan, M. and Lin, Y. (2006) Model selection and estimation in regression with grouped variables *Journal of the Royal Statistical Society: Series B (Statistical Methodology)*, 68(1):49–67
- Zou, H. (2006) The adaptive lasso and its oracle properties *Journal of the American Statistical Association*, 101(476):1418–1429.